CI&CEQ
Chemical Industry & Chemical Engineering Quarterly

Available on line at
Association of the Chemical Engineers of Serbia *AChE*
www.ache.org.rs/CICEQ

Chem. Ind. Chem. Eng. Q. 22 (2) 155–165 (2016) CI&CEQ

SAFIYE BAĞCI
AYHAN ABDULLAH CEYHAN

Selcuk University, Department of Chemical Engineering, Konya, Turkey

SCIENTIFIC PAPER

UDC 66.081.3:661.183:544.4

DOI 10.2298/CICEQ150522030B

ADSORPTION OF METHYLENE BLUE ONTO ACTIVATED CARBON PREPARED FROM *Lupinus albus*

Article Highlights

- Activated carbon was prepared from *Lupinus albus* by zinc chloride activation
- Activated carbon was used to remove methylene blue from aqueous solutions
- Surface area of 1254 m^2/g was characterized for activated carbon
- Maximum MB capacity of 109.89 mg/g was reported
- The kinetic data were well described by pseudo-second-order model

Abstract

The adsorption of methylene blue (MB) from synthetic aqueous solutions in batch experiments using Lupinus albus-activated carbon (LAAC) by chemical activation with zinc chloride was investigated. Prior to adsorption experiments, surface/physical properties of LAAC were determined using scanning electron microscopy, Fourier transform infrared spectroscopy and nitrogen adsorption isotherm. In the adsorption experiments, effects of adsorption time, solution pH, MB concentration and amount of LAAC were investigated. The isotherm and kinetic parameters were used to describe the experimental data. The BET surface area was 1254 m^2/g while its total pore volume was found to be 0.484 cm^3/g. Maximum adsorption capacity occurred at solution pH value 10 and was recorded as 109.89 mg/g. Adsorption data were modeled using Langmuir, Freundlich and Temkin adsorption isotherms. Langmuir isotherm and pseudo-second-order models fit to the process and reaction kinetics correspondingly.

Keywords: activated carbon, adsorption, Lupinus albus, methylene blue, zinc chloride.

Activated carbon is a carbon based amorphous material having high surface area and high porosity. Due to its high adsorption capacity, activated carbon has a wide range of applications, mostly used as a removing agent for both organic and inorganic materials [1].

There are two basic methods used in activation of activated carbon: chemical activation and physical activation. The natures of the raw materials, impregnation time and ratio, nature of the chemical activator, activation time and temperature have direct impact on the micro- and macro-porosity of the prepared activated carbon [2].

Correspondence: A.A. Ceyhan, Selcuk University, Department of Chemical Engineering, Konya, Turkey
E-mail: bagcisafiye@gmail.com; ceyhan@selcuk.edu.tr
Paper received: 22 May, 2015
Paper revised: 3 July, 2015
Paper accepted: 31 July, 2015

There is an increasing trend in environmental and water pollution due to the advancements in industrial fields. One of the sources of environmental and water pollution is anionic and cationic dyes. The presence of these waste dyes affects the life of a number of organisms in nature. Dyes are used as coloring material in many industries such as textile, leather, cosmetics, pulp and paper, plastics, pharmaceuticals and food industry (3). Dye residues from paint and other industries are among the basic causes of coloring observed in waste water. These residues in waste water are carcinogenic [3,4]. Relatively mild concentrations of the dyes are capable of coloring a huge amount of water and their removal is costly. This tends to limit subsequent use of the waste water in other fields [3,4].

When the toxic effects of dyes are taken into account, the importance of removing the materials from waste water becomes more vivid. Various physical, chemical and biological waste water purification

methods are used. One of these purification methods is adsorption. Due to its inert nature towards toxin impurities, ease of design, being user friendly and incurring lower establishing costs, adsorption has become one of the most preferred methods in removing dyes [5].

The activated carbon used in adsorption process can be obtained from various sources. Due to the high production costs, production methods that involve cheap raw materials are preferred. Recently, agricultural and industrial by-products have been investigated and found to be favorable for the preparation of activated carbon.

Lupinus albus (LA) plant is mostly grown in the Mediterranean and North America. In Turkey, the plant is grown in Ege, Marmara, inner-Anatolia and around the Mediterranean zones. These seeds of LA are used in production of pharmaceuticals and as animal feeds [6]. Used seeds of this plant are directly disposed. To our knowledge, there is no study that deals with LA plant seeds being used for preparation of activated carbon.

In this study, for the first time, LA plant was used in preparation of activated carbon. By using the obtained LAAC, removal of the MB from the aqueous solution was studied.

EXPERIMENTAL

Materials

The LA plant seeds were obtained from Konya region-Turkey. The seeds were ground (Retsch SR 300) and classified (Retsch AS200) based on their respective particle sizes. The particles with sizes under 250 μm were used for preparation of activated carbon. Then, they were washed with de-ionized water, dried at 105 °C for 48 h and stored in an enclosed container ready to be used in the preparation of activated carbon. During the experiments, deionized water and chemicals at analytical purity were used. MB was selected for adsorption experiments because of its known strong adsorption onto solids. MB dye was purchased from Merck Chemicals Company, Turkey. MB ($C_{16}H18N_3SCl$, molecular weight, 319.85 g/mol, wave length, 668 nm) was used without further purification.

Preparation of LAAC

First, thermogravimetric analysis (TGA) of the LA plant seeds considered for the preparation of LAAC was carried out. Thermogravimetric analysis was performed using a Perkin Elmer TG/DTA 6300. A 10±0.5 mg LA plant sample was carbonized to be heated from ambient temperature to 900 °C in N_2 atmosphere with a flow rate of 40 ml/min, at a linear heating rate of 10 °C/min. The test was carried out at least twice to decrease the test error, and good reproducibility was established. The DTG curve was derived from the TG curve.

In obtaining activated carbon, the chemical activation method with zinc chloride was used. The activation process was carried out in a tube furnace having inner diameter of 6 cm and a heat zone of length of 25 cm (Magma Therm MTTF12/75/600-E-4). After mixing the raw material (5 g) with zinc chloride at the ratio of 1:1, 1:3, 1:5, 1:7 and 1:9 (g raw material/g zinc chloride activator), 20 ml of de-ionized water was added after which impregnation took place for periods of 6, 12, 24, 48, 72, 96 and 120 h. The impregnated raw materials were subjected to activation process, which was carried out at the heating rate of 10 °C/min. under operating temperatures of 350, 400, 500 and 600 °C. The activation periods were selected to be 15, 30, 45 and 60 min. The activation and cooling processes were completely accomplished under N_2 gas medium. In order to rinse the zinc compounds off the obtained activated carbons and open blocked pores, the activated carbons were washed with 0.5 M HCl acid. Then, the rinsing of the LAAC with hot de-ionized water was prolonged until the solution pH value became the same as that of de-ionized water.

In this study, the activated carbon obtained from the conditions of impregnation ratio of (1:7), impregnation time of 48 h, activation temperature of 400 °C and activation time of 30 min was used.

Sample characterization

Prediction of the specific surface area, porosity volume and porous diameter of the LAAC was done with BET device (Quantachrome Nova 1200), whereas the micro porosity volume was calculated by using the t-plot micro porosity volume method. Distribution of the porosity sizes was specified by making use of the Barret-Joyner-Halenda (BJH). The porosity structure and surface morphologies of the LAAC obtained were found by using an SEM device (Zeiss Evo/LS 10). The surface chemistry was characterized by determination of surface acidity/basicity with FT-IR spectroscopy (Perkin Elmer 1100 series FT-IR device at the range of 4000-400 cm^{-1} by using KBr pallets at an accuracy of 1 cm^{-1}). Zeta potential measurements were also carried out using a Malvern Zeta-sizer Zen 3600.

Adsorption experiments

During the adsorption process, 0.2 L solutions of MB having initial concentrations that range from 50 to 300 mg/L were used. The experiments were conducted into a thermostatic shaker (Memmert WNB 7-45) and at constant temperature of 30 °C. At the beginning, the solution temperature was taken to be 30 °C, whereas the initial solution concentration was set at 100 mg/L. The adsorption of MB onto LAAC was investigated as a function of time in order to find out the equilibrium time for maximum adsorption capacity. Optimum adsorption time intervals for different pH values ranging between 2 to 10 were determined. Samples were taken from the solution (range: 0--180 min) and the concentrations were determined. With the given optimum adsorption time and pH values, effects of the amount of LAAC having weight range of 0.05 to 0.5 g on the adsorption process were studied. At the end of the adsorption process, a UV spectrophotometer (Biochrom Libra S22 UV) was used to determine the concentrations of MB in the solution. The amount of MB adsorbed by the adsorbent at equilibrium, q_e (mg/g), is calculated by using Eq. (1) below:

$$q_e = \frac{(c_0 - c_e)}{w} V \tag{1}$$

where c_0 (mg/L) is the initial concentration of MB in the solution, c_e (mg/L) is the concentration of MB in the solution at equilibrium, q_e (mg/g) is the amount of MB adsorption at equilibrium, and V (L) is the solution volume.

RESULTS AND DISCUSSION

First, 10 mg sample was carbonized to be heated from ambient temperature to 900 °C. Experiment was conducted under the N_2 atmosphere. DTG curve was derived from TG curve. The temperature of activated carbon preparation was determined as 400 °C by using DTG curve. Thermogravimetric analysis (TGA, DTG) of the LA plant under N_2 atmosphere are shown in Figure 1.

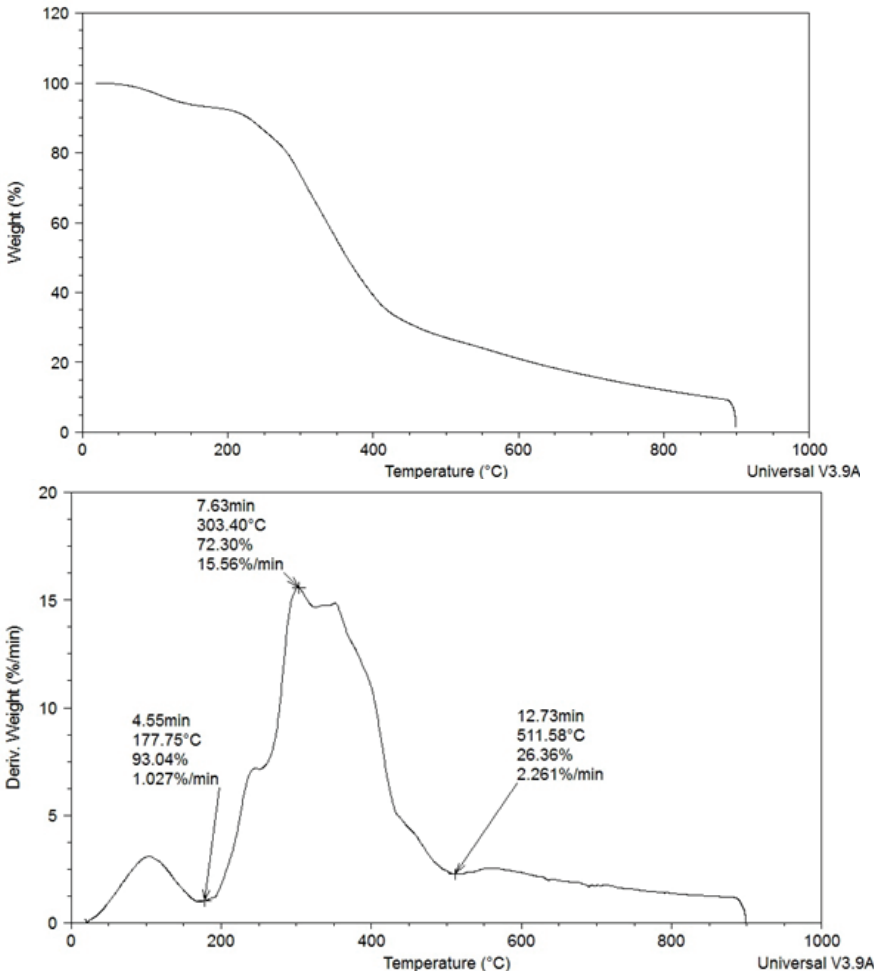

Figure 1. The TG and DTG graphs of LA plant seeds.

TG and DTG curves for LA plant seed are illustrated in Figure 1. The TG curve shows the percentage loss of mass for LA plant seeds at different temperatures. It can also be observed the thermal decomposition of seeds take place in two steps. The TG curves for the 10 °C/min. heating rate shows a gradual weight loss starting at 50 °C temperature and ending at about 177 °C with a DTG peak at 100 °C. The total loss of weight up to 177 °C is related to the loss of absorbed water by LA plant seeds. One broad peak is observed in the temperature range from 177 up to 511 °C with a DTG peak at 303 °C. The total loss of weight up to 511 °C is related to pyrolysis of PA plant seeds. The DTG curve is identical to the TG curve as well. According to the TG and DTG results, the thermal decomposition of LA plant seed can be written as follows;

$$LA_{seed} \cdot xH_2O \xrightarrow{50-177\ ^\circ C} LA_{seed} + xH_2O_{(gas)} \quad (I)$$

$$LA_{seed} \xrightarrow[80\%\ \text{weight loss}]{177-511\ ^\circ C} LAAC_{solid} + XY_{(gas)} \quad (II)$$

As shown in *n* reaction steps above, the thermal decomposition of LA plant seeds (LA_{seed}) can be subdivided into two main stages – dehydration and pyrolysis, respectively. In the first step, the absorbed water exists in the LA plant seeds at the low temperature range. In the next step, pyrolysis of LA plant seeds occurs at high temperature range from 177--511 °C, resulting in the formation of LAAC. Different gases compounds are represented as $XY_{(gas)}$.

The FT-IR spectrum given in Figure 2a presents functional groups found in the structure of pure and LAAC obtained with a 2-day chemical activation with 350% $ZnCl_2$ at 400 °C. According to the given spec-

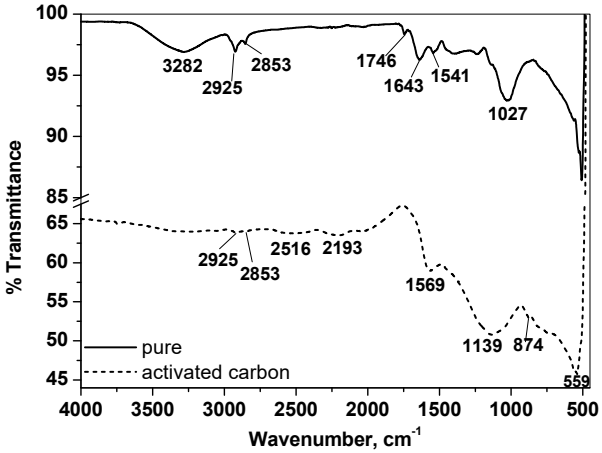

(a)

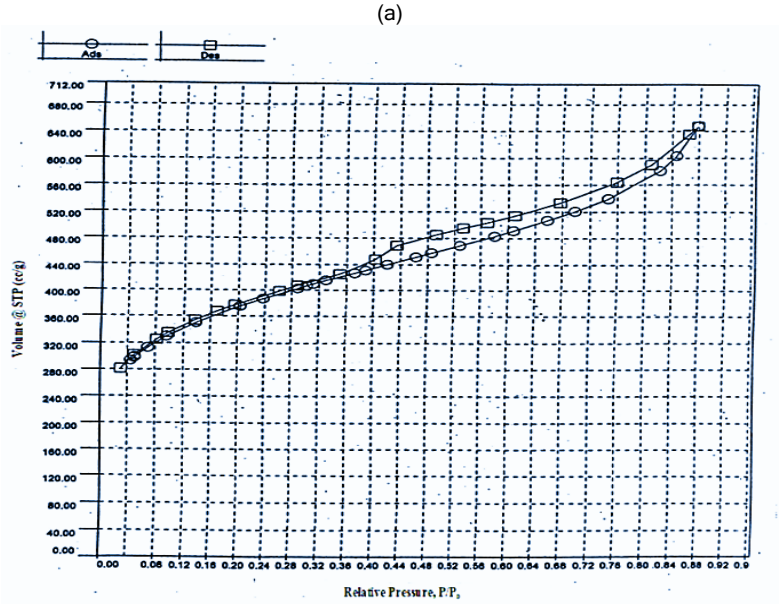

(b)

Figure 2. a) FT-IR spectra for the activated carbon obtained at 400 °C temperature, 1:7 impregnation ratio, 48 h of impregnation time and 30 min of activation period; b) N_2 gas adsorption and desorption isotherm at -196 °C for the activated carbon obtained at 400 °C temperature, 1:7 impregnation ratio, 48 h of impregnation time and 30 min of activation period.

trum, the spread peak seen in the band ranging between 3200 and 3600 cm^{-1} is caused by the –OH stretching vibration mode of the hydroxyl functional groups. This is generally caused by the moisture found in the shell structure. The peaks observed at 2900 and 2800 cm^{-1} band indicate the aliphatic groups found in the structure of the LA shells. The peaks observed at 1750 cm^{-1} show carbonyl (C=O) stretching, which indicates that there might be derivatives of aldehyde, ketone and ester. The peaks observed at about 1650 cm^{-1} were caused by the stretching of the C=C structure. The peak found at about 1100 cm^{-1} in the spectrum is caused by the C–O stretching which indicates possible existence of the acids, alcohols, phenols, ethers and esters in the raw material.

When the spectrum of the produced LAAC was compared with the FT-IR spectrum of the original walnut shell specimen, substantial changes in the functional groups were found [7]. At around 3400 cm^{-1} band, the observed maxima resulted from the –OH stretching disappeared completely. Even the peaks observed at 2900 and 2800 cm^{-1} that show aliphatic groups existing in the LA structure were not in the structure of the LAAC. However, the peaks observed at 1600 and 1100 cm^{-1} were found to have increased their intensities.

In Figure 2b, isothermal absorption and desorption of N_2 gas at -196 °C, for the LAAC were obtained by setting operating conditions at 400 °C, impregnation ratio of 1:7, impregnation time of 48 h and activation time of 30 min. According to the IUPAC classification, these types of isotherms cope with the type IV isotherm class. This situation can be described with the narrow outlet discharging. Generally, adsorption isothermals on micro- and mezzo-porous layers resemble this type [8]. The surface area and micropore volume of the LAAC prepared are 1254 and 0.3584 cm^3/g, respectively. The average width of the LAAC's BJH adsorption is 1.54 nm. This result indicates that the average porous width for the BJH adsorptionis of micro type.

SEM photographs of the LAAC are shown in Figure 3. As seen from the SEM images, with well-developed pores, the obtained LAAC has a random and heterogeneous surface. The surface of the LAAC has cracks, grooves and large pores. In addition, pores of different sizes are also present.

Adsorption studies

Effect of pH

The adsorption procedures started with the investigation of effects of solution pH. The studies were carried out at a constant temperature of 30 °C in MB concentration of 100 mg/L and with 0.1 g of the LAAC. The solution pH was varied between 2 and 10. The results obtained are presented in Figure 4a.

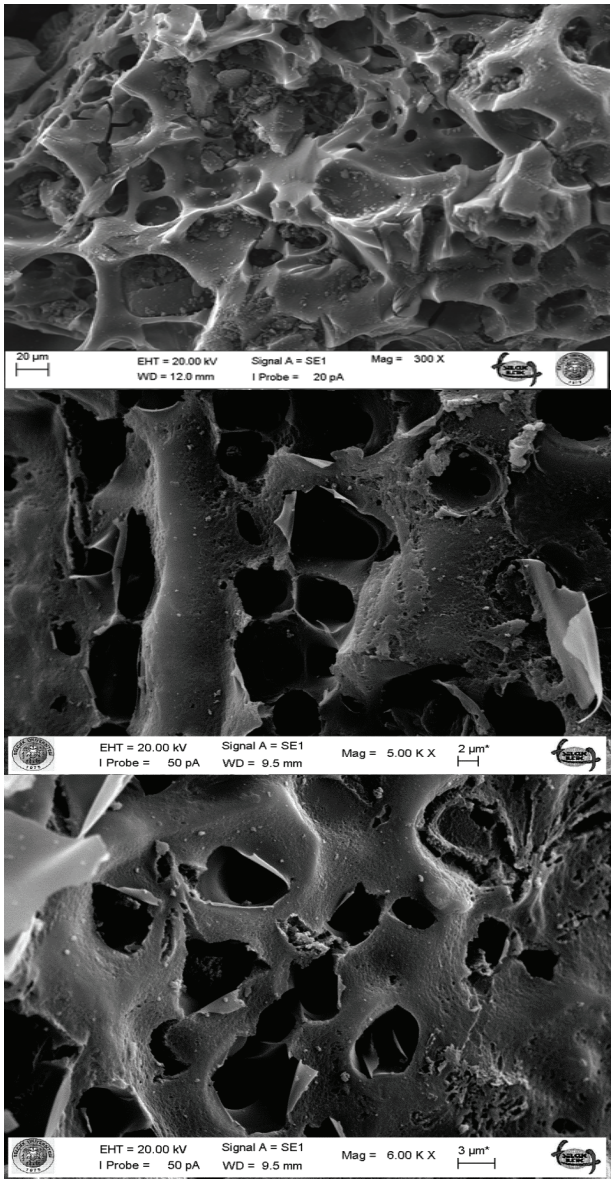

Figure 3. SEM views of the produced activated carbon.

The increase in solution pH from 2 to 10 has led to significant increase in the adsorption capacity. The most probable reason for this increase is the pH dependent electrostatic interaction between the activated carbon and the MB molecules. When the solution pH increased from 2 to 10, the adsorption capacity of the activated carbon increased from 45.19 to 89.80 mg/g. As for the adsorption of the MB, the presence of two possible mechanisms may be pronounced. These are:

- electrostatic interaction between MB molecules and positively charged groups of the activated carbon and
- chemical reaction between the adsorbent and the MB molecules.

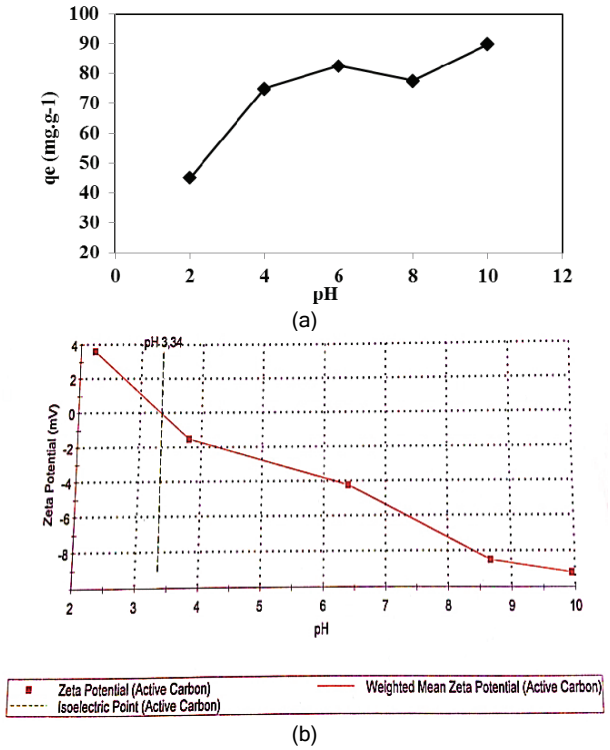

Figure 4. a) Variation of the adsorption capacity, q_e, with solution pH (T: 30 °C, MB concentration: 100 mg/L, LAAC mass: 0.1 g); b) the point of zero charge values.

Activated carbon is amphoteric in nature. Its surface electrical charge can vary between positive and negative depending on the solution pH [9]. The point at which the net charge of adsorbent is equal to zero (pH_{PZC}) can be used to characterize the effect of pH. It means smaller pH solution of adsorbent than pH_{PZC} results positive surface and bigger one negative surface. Variation of surface charge of the LAAC with pH was investigated and the results are as shown in Figure 4b. The adsorption of the MB onto the LAAC having cationic character is more remarkable if it acquires the condition that is pH > pH_{PZC} (point of zero charge) which is equal to 3.14.

When the solution pH is low, the H^+ relocate themselves into active surface sites onto the activated carbons and hence prevent adsorptions of the MB molecules having cationic characters. With increasing pH, the surface charge reaches a zero point of charge (pH_{PZC}), which is the zero net charge of adsorbents (at pH values of 3.14). After this point, an increase in pH value leads to the increase of negative character of the activated carbon surface and increase in the adsorption of the MB [10-12]. Other researchers also found that the optimum solution pH value in removing of MB with activated carbon is 10 [9,13-17].

Effect of contact time

Contact time varies with respect to features such as the pore diameter, volume and surface areas of activated carbon [12]. In this section of the study, efforts have been made to determine adsorption capacity at equilibrium by maintaining parameter values such that pH is at 10, the amount of LAAC is 0.1 g, solution temperature is kept at 30 °C and concentration is kept at 100 mg/L (Figure 5a). It was found that the maximum adsorption capacity for the MB at the end of 120 min interval is 89.80 mg/g. The amount of MB adsorbed increases with the contact time and at the onset of the 120th min, the amount reaches its equilibrium value.

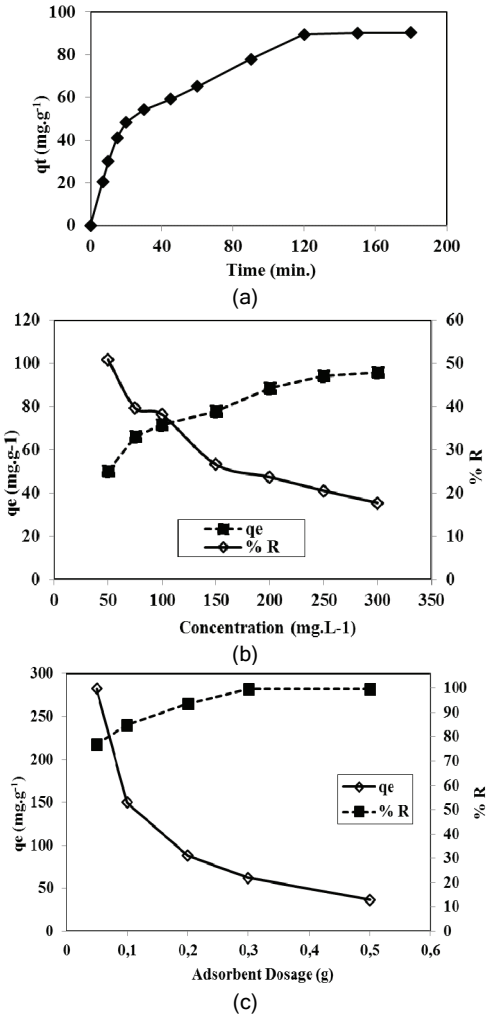

Figure 5. a) Time for the adsorption to reach equilibrium; b) effects of initial MB concentration on adsorption; c) effects of the amount of activated carbon used on adsorption of MB (T: 30 °C, MB concentration: 100 mg/L, pH 10, contact time: 120 min).

During adsorption process from the solution to the surface of the activated carbon, the followings happen:

- transfer of MB molecules from the solution to the solution-adsorbent boundary layer,
- diffusion from boundary layer to the adsorbent surface,
- diffusion phases from adsorbent surface into its pores [15].

The results show that the adsorption process occurs faster at the beginning of the contact time (≈40%). However, the process proceeds gradually step by step towards equilibrium value. The vacant active surface sites on the surface fill quickly as the adsorption process starts. As the number of vacant active surface sites on the surface decreases with time and the diffusion rate attenuates, the time to reach equilibrium tends to increase [18].

Effect of initial MB concentration

In this section of the study, effects of MB solutions with concentrations of 50, 75, 100, 150, 200, 250 and 300 mg/L on the adsorption capacity of LAAC are investigated. Figure 5b shows variation of the initial concentration of MB with the amount of MB adsorbed by the LAAC. It is seen that when equilibrium is reached, adsorption capacity becomes greater for higher initial concentrations. At higher initial concentrations, mass transfer resistance between solid surface and solution is easily overcome. With increasing MB concentration, vacant active surface sites on the adsorbent surface tend to fill quickly. However, the rate of removal percentage of the MB (*R%*) is inversely proportional to the increasing initial concentration. For low initial concentration, competition of MB molecules for adsorption to the surface is at much lower rates [19]. Moreover, the adsorption equilibrium is achieved more quickly. Even the ratio of MB concentration in the solution to the number of active sites on the adsorbent is lower. That's why the concentration of removed MB becomes higher [12]. Similar to the results of this study, in studies conducted on removal of MB by using activated carbons, it was determined that with the increasing solution concentration, the removal percentage of the MB tends to fall [20-22].

Effect of adsorbent dosage

The size, amount and pore volume of the activated carbon used in the adsorption are among the most important parameters. As the amount of activated carbon increases, the surface area tends to increase and hence adsorption capacity also increases. In this phase of the study, the operating conditions specified previously (100 mg/L, 30 °C, pH 10, contact time 120 min) were kept constant and the experiments were conducted (Figure 5c). The amount of LAAC used was varied between 0.05 and 0.5 g. By increasing the amount of LAAC to 0.3 g, the removal percentage of the MB jumps to a value of 99%. However, beyond this point, additional LAAC was found to have no significant effects in removing the MB. Another result indicates that the adsorption capacity (q_e) deteriorates substantially with the increasing amount of activated carbon. Possible reasons for this are the presence of more vacant active surface sites in the medium than the MB concentration needs, lowering of surface area as a result of accumulation of adsorbent particles, and elongation of the path to be taken during the diffusion step [12,23].

Adsorption isotherms

Adsorption isotherms play an important role in estimating real time adsorption capacities of adsorbents of different nature. The equilibrium values obtained after the adsorption of MB were investigated by using Langmiur, Freundlich, Temkin and Dubinin–Radushkevich isotherms. The adsorption data obtained experimentally are given in Figure 6 and Table 1.

The Langmuir isotherm assumes that there is a certain number of active surface sites with similar features on the surface. These centers are evenly distributed over the surface and the adsorption is of a monolayer type [24]. The theory can be represented by the following linear form:

$$\frac{c_e}{q_e} = \frac{1}{q_m K_L} + \frac{c_e}{q_m} \tag{2}$$

$$R_L = \frac{1}{1 + K_L c_0} \tag{3}$$

where c_e is equilibrium concentration (mg/L), q_e is the amount adsorbed at equilibrium (mg/g), K_L is a constant related to adsorption energy and capacity (L/mg), q_m is the monolayer adsorption capacity (mg/g) and c_0 refers to initial concentration of the solution (mg/L). The separation factor (R_L) which the basic characteristic of the Langmuir adsorption isotherm is calculated by using Eq. (3). The R_L value between 0 and 1 indicates that the activated carbon is favorable for using MB adsorption [25]. The R_L values found for different initial concentrations were in the range $0 < R_L < 1$. This result shows that the activated carbon prepared from LA plant for adsorption of MB is favorable.

The Freundlich isotherm assumes that the surface possesses heterogeneous energy distribution. This isotherm, which also covers intra-molecular inter-

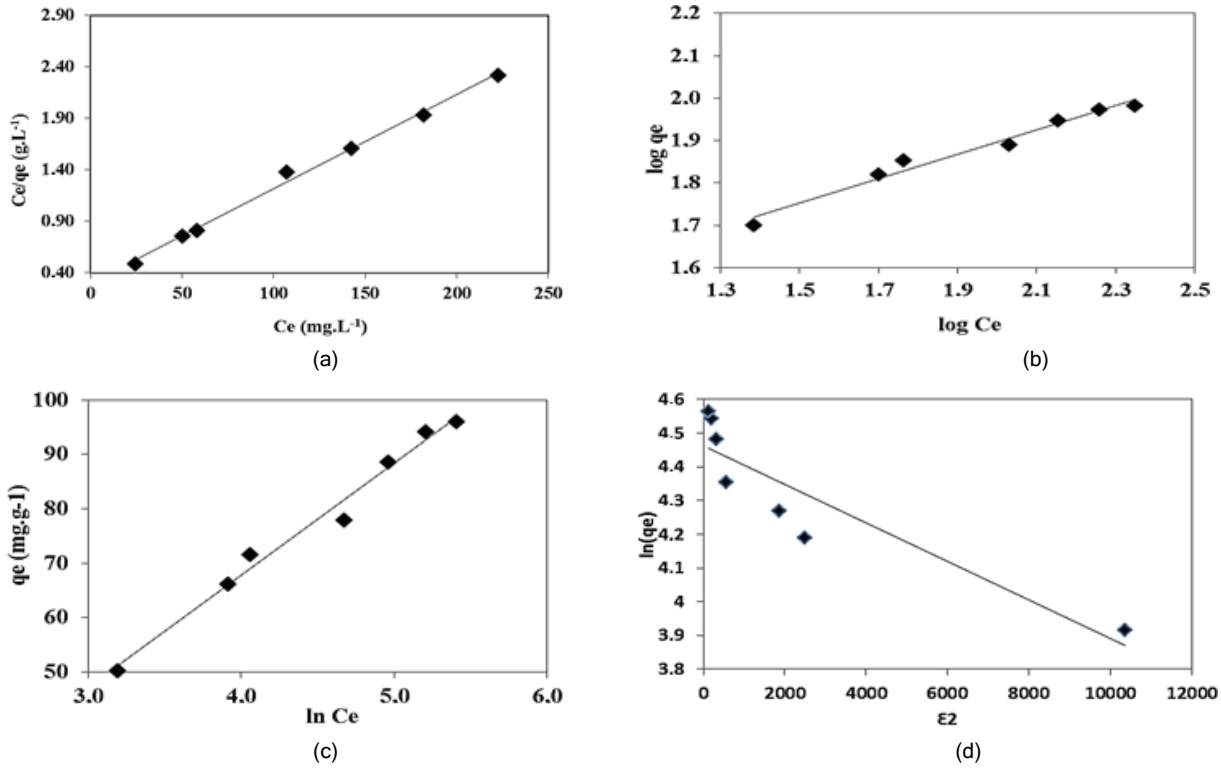

Figure 6. Adsorption isotherms: a) Langmuir, b) Freundlich, c) Temkin and d) D-R.

Table 1. Isotherm constants for the adsorption isotherm models

Isotherm	Isotherm constants		
Langmuir	q_{max} = 109.89 mg/g	K_L = 0.03	R^2 = 0.995
Freundlich	K_f = 21.09 (mg/g)(mg/L)$^{1/n}$	n = 3.51	R^2 = 0.974
Temkin	K_t = 0.486 L/g	B = 122.053 J/mol	R^2 = 0.984
Dubinin-Radushkevich	q_m = 86.606 mg/g	E = 93 J/mol	R^2 = 0.829

action, is favorable for heterogeneous systems; and instead of monolayer adsorption, it takes the possibility of multilayer adsorption into account.

$$q_e = K_f c_e^{1/n} \quad (4)$$

In Eq. (4), K_f is a constant for the system, related to the bonding energy and n is the adsorption intensity, which is used to account for the adsorption process is favorable. $1/n$ is a measure of adsorption intensity or surface heterogeneity. A higher value of adsorption capacity K_f indicates that the capacity of the prepared activated carbon is high, whereas higher adsorption intensity, n, indicates that the adsorption process takes place thoroughly throughout the concentration interval of solution employed. Lower n value at higher initial MB concentration implies that the adsorption occurs perfectly. As for lower initial MB concentrations, it can be said that there is a little correlation between experimental data and the Freundlich isotherm.

In Table 1, n and K_f constants for the Freundlich isotherm are presented. The adsorption intensity (n) was calculated to be 3.51. This result shows that the activated carbon prepared is favorable for the high MB concentration. The value of $1/n$ = 0.289, being in the range of $0.1 < 1/n < 1$, indicates favorably of the prepared activated carbon for adsorption process [26].

The Temkin isotherm is similar to the Freundlich isotherm as it also takes intra-molecular interaction into account. It is with the image that if the heat of adsorption for all molecules covers the surface perfectly, then the heats must fall linearly. The postulate, in addition, considers that binding energy is distributed uniformly to the maximum value.

$$q_e = B \ln K_t + B \ln c_e \quad (5)$$

$$B = RT / b \quad (6)$$

In Eqs. (5) and (6), b is the Temkin isotherm constant (J/mol), K_t is the equilibrium binding constant

corresponding to the maximum binding energy (L/g), B is a dimensionless constant related to heat of adsorption, R is the ideal gas constant (8.314 J/(mol K)), T is the temperature of the medium (K).

The Dubinin-Radushkevich isotherm aims at establishing the view that adsorption occurs either physically or chemically. Based on this isotherm, it is described that if the average adsorption energy is lower than 8 kJ/mol, then physical adsorption takes place, and if it is between 8 and 16 kJ/mol then ion variation adsorption occurs, whereas higher adsorption energy values is characterised by chemical adsorption [13].

$$B \ln q_e = \ln q_m - k\varepsilon^2 \tag{7}$$

$$\varepsilon = RT \ln(1+1/c_e) \tag{8}$$

$$E = (2k)^{-1/2} \tag{9}$$

In Eqs. (7)-(9), q_s is denoted as the theoretical isotherm saturation capacity(mg/g), ε is the Polanyi potential (J/mol), k is the activity coefficient (J^2/mol^2), and E is the mean free energy (J/mol). The calculated mean free energy (E) value was smaller than 8 kJ/mol. This result shows that physical interaction between the adsorbent and the adsorbate is dominant and that the process occurred by physical adsorption.

As shown in Table 1, the largest correlation coefficient (R^2) is from the Langmuir isotherm. The phenomenon implies that the removal of the MB is well described by the Langmuir isotherm. In addition, it also indicates that the adsorption has essentially taken place in a monolayered form. However, due to energy distribution discrepancies on the surface, some sites were marked with multi-site adsorption [27].

Adsorption kinetics

In this section of the study, kinetic behaviors of the adsorption process are taken into consideration by making use of the adsorption experimental data. With this aim, three different kinetic models were used, namely, the pseudo-first-order, pseudo-second-order and intraparticle diffusion model.

The variation of the adsorption capacity with time of the pseudo-first-order model developed by Lagergren and Svenska [28] is described by Eq. (10):

$$\frac{1}{q_t} = \frac{1}{q_e} + \frac{k_1}{q_e}\frac{1}{t} \tag{10}$$

where k_1 is the apparent kinetic rate constants of first-order reaction kinetic (min^{-1}) and t is the reaction time (min).

The variation of adsorption capacity with time in the pseudo-second-order model developed by Ho and McKay [29] is expressed by Eq. (11):

$$\frac{t}{q_t} = \frac{1}{k_2 q_e^2} + \frac{1}{q_e}t \tag{11}$$

where k_2 is the apparent kinetic rate constants of second-order reaction kinetic (g/(mg min)).

The intraparticle diffusion model developed by Weber and Morris [30] is expressed by Eq. (12):

$$q_t = k_{id} t^{1/2} + C \tag{12}$$

where k_{id} is the intraparticle diffusion rate constant (mg/(g $min^{1/2}$)), and C is a constant that gives an idea about the thickness of the boundary layer (mg/g). If intraparticle diffusion is involved in the overall adsorption process, the plot of uptake (q_t) *versus* the square root of time ($t^{0.5}$) should be linear. Moreover, if this line passes through the origin, the intraparticle diffusion is the rate controlling step of the process. If the plots do not pass through the origin, it points out of some degree of boundary layer control. Besides, it shows that the intraparticle diffusion is not the only rate-limiting step, but also other kinetic models may control the rate of adsorption process.

These plots usually are depicted as three stages such as curve, linear and plateau in turn. The initial stage is caused by external mass transfer. The intermediate linear stage is caused by intra-particle diffusion. The last plateau stage where intraparticle diffusion starts to slow down is caused by extremely low solute concentrations in the solution [31]**.** The adsorption graphs of the models considered in the study are given in Figure 7.

When deciding on the validity of a model, besides the correlation coefficient (R^2), closeness of the adsorption capacities (q_e) is evaluated as well [32]. The normalized standard deviation Δq is calculated using the following equation:

$$\Delta q = 100\sqrt{\frac{\left[\left(q_{exp} - q_{cal}\right)/q_{exp}\right]^2}{N-1}} \tag{14}$$

Values of Δq for the pseudo-first-order model, pseudo-second-order model and the intraparticle diffusion model as well as kinetic parameters were calculated and presented in Table 2.

From Table 2, the largest correlation value (0.999) and the lowest normalized standard deviation (1.002) occur on the pseudo-second-order model. More concentrations (50 and 150 ppm) were used to establish the kinetics models. Similar results were found for 100 pm (figures not shown).

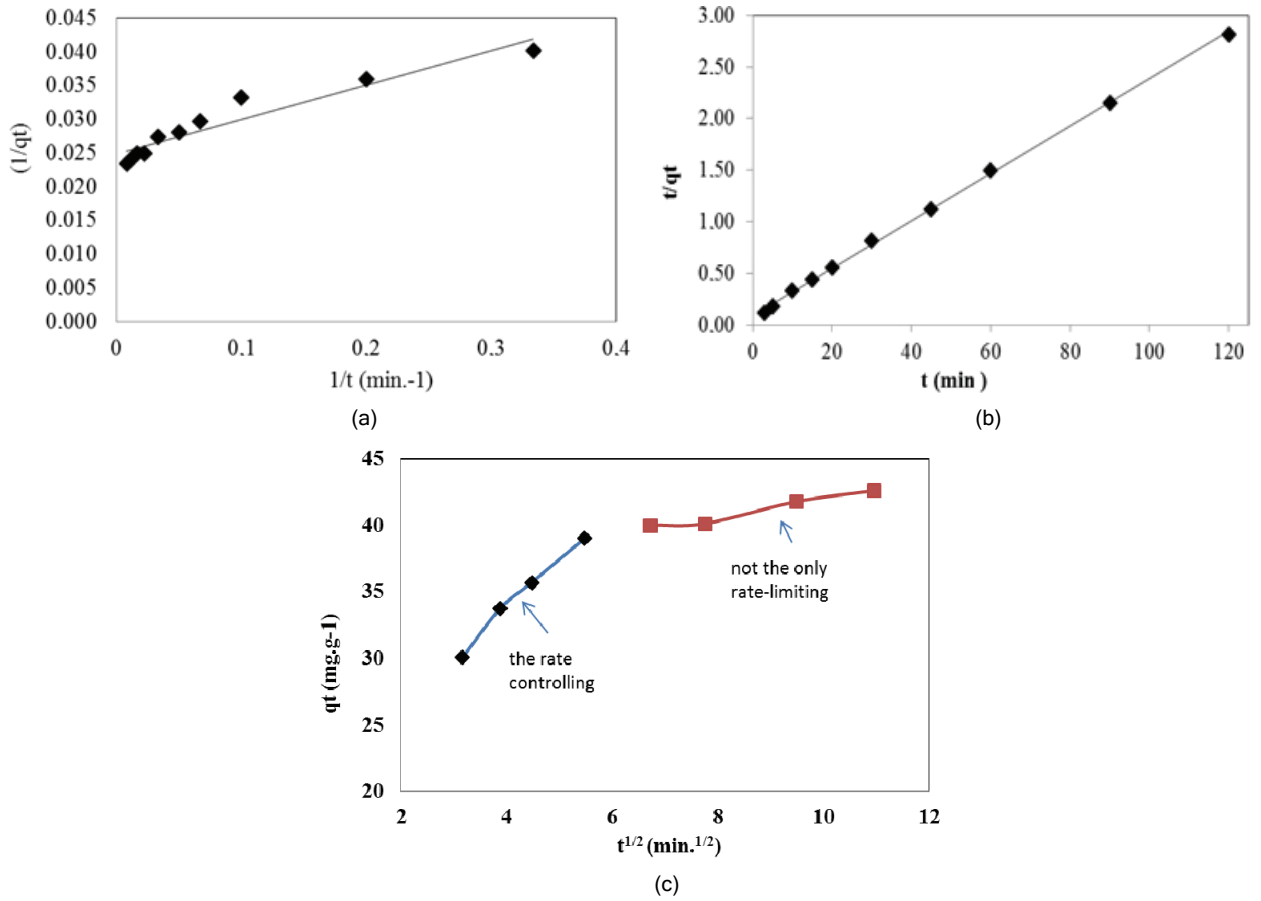

Figure 7. Adsorption kinetic models: a) pseudo-first order, b) pseudo-second order, c) intra-particle model (T: 30 °C, MB concentration: 100 mg/L, LAAC mass: 0.1 g, pH: 10, contact time: 120 min).

The pseudo-second-order model assumes that the dominant process is chemical adsorption, and that there are chemical electrostatic interactions between the adsorbent surface and the adsorbate. The surface is monolayered but it is most likely that some sites can be multilayered as well [32].

The intra-particle diffusion model (Weber-Morris model) is widely used for the purpose of determining the rate-specifying stage. On the graph of intraparticle diffusion model, though the variation is almost linear, and the lines do not cross the origin. This phenomenon indicates that the adsorption is not only rate-controlled but also a boundary layer diffusion controlled. In addition, it infers to macroporous diffusion and suggests that the active surface sites on the surface fill up quickly [33]. The calculated α value was found to be 0.12. The value of α being smaller than 0.5 indicates that the intraparticle diffusion is not the only step that depicts diffusion rate [34].

CONCLUSION

In this study, activated carbons were prepared from LA plant by using chemical activation with $ZnCl_2$ under N_2 gas atmosphere. Effects of parameters like impregnation ratio, impregnation time, activation temperature and activation time were studied. The impregnation ratio of 1:7 and impregnation time of 48 h were selected. Activation temperature and activation time were 400 °C and 30 min, respectively. The BET surface area of the LAAC was determined to be 1254 m^2/g. Micropore volume of the activated carbon was found to be 0.3584 cm^3/g based on the t-plot method. According to the BJH adsorption average, the porous diameter is 1.54 nm. During the adsorption process it was also found that the maximum adsorption capacity is 109.89 mg/g and occurs at pH value of 10. It was found favorable to describe the adsorption based on the Langmuir isotherm. As for the reaction kinetics, the pseudo-second-order model was found to be a convenient match.

Acknowledgements

This study has been financially supported by the Office of Scientific Projects Coordinator of Selcuk University (BAP) (Project No: 12201090).

REFERENCES

[1] J. Kong, Q. Yue, L. Huang, Y. Gao, Y. Sun, B. Gao, Q. Li, Y. Wang, Chem. Eng. J. **221** (2013) 62-71

[2] M.O. Abdullah, I.A.W. Tan, L.S. Lim, Renewable Sustainable Energy Rev. **15** (2011) 2061-2072

[3] M. Rafatullah, O. Sulaiman, R. Hashim, A. Ahmad, J. Hazard. Mater. **177** (2010) 70-80

[4] M. Arulkumar, P. Sathishkumar, T. Palvannan, J. Hazard. Mater. **186** (2011) 827-834

[5] M. Berrios, M.A. Martín, A. Martín, J. Ind. Eng. Chem. **18** (2012) 780-784

[6] O. Güldemir, N. Işık, F. Tosun, Sokaklardan evlere: Termiye, 3. Geleneksel Gıdalar Sempozyumu, Konya, Turkey, 2012, p. 549

[7] M. Kılıç, E.A. Varol, A.E. Pütün, Appl. Surf. Sci. **261** (2012) 247-254

[8] Y. Sarıkaya, Fizikokimya, Gazi Kitabevi, Ankara, 2000, p. 633

[9] Y. Bao, G. Zhang, Energy Procedia **16** (2012) 1141-1146

[10] G. Mezohegyi, F.P. van der Zee, J. Font, A. Fortuny, A. Fabregat, J. Environ. Manage. **102** (2012) 148-164

[11] K. Gobi, M.D. Mashitah, V.M. Vadivelu, Chem. Eng. J. **171** (2011) 1246- 1252

[12] M. Ghaedi, A.G. Nasab, S. Khodadoust, M. Rajabi, S. Azizian, J. Ind. Eng. Chem. **20** (2014) 2317-2324

[13] C. Saka, Ö. Şahin, Color. Technol. **127** (2011) 246-255

[14] H. Cherifi, B. Fatiha, H. Salah, Appl. Surf. Sci. **282** (2013) 52-59

[15] S. Senthilkumaar, P.R. Varadarajan, K. Porkodi, C.V. Subbhuraam, J. Colloid Interface Sci. **284** (2005) 78-82

[16] H. Deng, L. Yang, G. Tao, J. Dai, J. Hazard. Mater. **166** (2009) 1514-1521

[17] M. Ertaş, B. Acemioğlu, M.H. Alma, M. Usta, J. Hazard. Mater. **183** (2010) 421-427

[18] M. Auta, B.H. Hameed Chem. Eng. J. **175** (2011) 233--243

[19] Z. Zhang, Z. Zhang, Y. Ferna´ndez, J.A. Mene´ndez; H. Niu, J, Peng, L. Zhang, S. Guo, Appl. Surf. Sci **256** (2010) 2569-2576

[20] F. Raposo, M.A. De La Rubia, R. Borja, J. Hazard. Mater. **165** (2009) 291-299

[21] Y. Guo, J. Qi, S. Yang, K. Yu, Z Wang, H. Xu, Mater. Chem. Phys. **78** (2003) 132-137

[22] M. Ghaedi, Sh. Heidarpour, S.N. Kokhdan, R. Sahraie, A. Daneshfar, B. Brazesh, Powder Technol. **228** (2012) 18--25

[23] J. Yang, K. Qiu, Chem. Eng. J. **165** (2010) 209-217

[24] A.W. Adamson, Physical Chemistry of Surface, Interscience Publication, New York, 1960, p. 603

[25] N. Kannan, M.M. Sundaram, Dyes Pigm. **51** (2001) 25-40

[26] T. Karthikeyan, S. Rajgopal, L.R. Miranda, J. Hazard. Mater. **124** (2005) 192-199

[27] Y. Gao, Q. Yue, B. Gao, Y. Sun, W. Wang, Q. Li, Y. Wang, Chem. Eng. J. **217** (2013) 345-353

[28] S. Lagergren, K. Sven, Vetenskapsakad. Handl. **24** (1898) 1-39

[29] Y.S. Ho, G. Mckay, Process Biochem. **34** (1999) 451-465

[30] W.J. Weber, J.C. Morris, J. Sanit. Eng. Div., Am. Soc. Civil Eng. **89** (1963) 31-59

[31] A.A.M. Daifullah, S.M. Yakout, S.A. Elreefy, J. Hazard. Mater. **147** (2007) 633-644

[32] S.K. Theydan, M.J. Ahmet, J. Anal. Appl. Pyrolysis **97** (2012) 116-122

[33] D. Kavitha, C. Namasivayam, Bioresour. Technol. **98** (2007) 14-21

[34] K.K. Singh, R. Rastogi, S.H. Hasan, J. Colloid Interface Sci. **290** (2005) 61-68.

SAFIYE BAĞCI
AYHAN ABDULLAH CEYHAN

Selcuk University, Department of Chemical Engineering, Konya, Turkey

NAUČNI RAD

ADSORPCIJA METILENSKOG PLAVOG NA AKTIVNOM UGLJU PRIPREMLJENOM OD *Lupinus albus*

U radu je analizirana adsorpcija metilenskog plavog (MB) iz vodenih rastvora u šaržnim eksperimentima na aktivnom uglju dobijenom od Lupinus albus (LAAC), koji je hemijski aktiviran cink-hloridom. Pre ispitivanja adsorpcije, površinske i fizičke osobine LAAC su određene elektronskom mikrosopijom, infracrvenom spektroskopijom sa Furijeovom transformacijom i adsorpcijom azota. U adsorpcionim eksperimentima istraživani su uticaji vremena adsorpcije, pH rastvora, koncentracije MB i količine LAAC. Na osnovu dobijenih eksperimentalnih podataka određeni su kinetički parmetri i parametri adsorpcionih izotermi. Specifična površina po BET metodi je bila 1254 m^2/g, dok je ukupna zapremina pora bila 0,484 cm^3/g. Maksimalni adsorpcioni kapacitet je 109,89 mg/g sa rastvorom čiji je pH 10. Eksperimentalni podaci su modelovani Lengmirovom, Frojndlihovom i Temkinovom adsorpcionom izotermom. Kinetika i ravnoteža adsorpcije slede model pseudo drugog reda i Langmuirovu izotermu, redom.

Ključne reči: aktivni ugalj, adsorpcija, Lupinus albus, metilensko plavo, cink--hlorid.